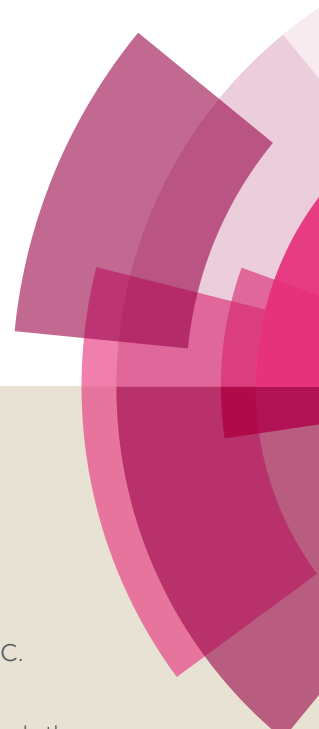


NJC

Accepted Manuscript



This article can be cited before page numbers have been issued, to do this please use: F. Scé, I. Cano, C. Martin, G. Beobide, O. Castillo and I. de Pedro, *New J. Chem.*, 2019, DOI: 10.1039/C8NJ06090H.



This is an Accepted Manuscript, which has been through the Royal Society of Chemistry peer review process and has been accepted for publication.

Accepted Manuscripts are published online shortly after acceptance, before technical editing, formatting and proof reading. Using this free service, authors can make their results available to the community, in citable form, before we publish the edited article. We will replace this Accepted Manuscript with the edited and formatted Advance Article as soon as it is available.

You can find more information about Accepted Manuscripts in the [author guidelines](#).

Please note that technical editing may introduce minor changes to the text and/or graphics, which may alter content. The journal's standard [Terms & Conditions](#) and the ethical guidelines, outlined in our [author and reviewer resource centre](#), still apply. In no event shall the Royal Society of Chemistry be held responsible for any errors or omissions in this Accepted Manuscript or any consequences arising from the use of any information it contains.

Comparing Conventional and Microwave-Assisted Heating in PET Degradation Mediated by Imidazolium-Based Halometallate Complexes†

View Article Online

DOI: 10.1039/C8NJ06090H

Fabio Scé,^a Israel Cano,^{*b} Carmen Martín,^b Garikoitz Beobide,^c Óscar Castillo^c and Imanol de Pedro^{*a}

ABSTRACT: The catalytic activity of two halometallate complexes based on imidazolium cation, (dimim)[FeCl₄] (**1**) and (dimim)₂[Fe₂Cl₆(μ-O)] (**2**), was evaluated in the glycolysis of polyethylene terephthalate (PET), either under conventional heating or microwave-assisted conditions. The two procedures led to the formation of bis(2-hydroxyethyl)terephthalate (BHET) as the major product with high yields, also allowing the isolation and structural characterization of a new polymorph. The influence of the halometallate structure on the catalytic activity was investigated, and additional experimental studies proved the involvement of both imidazolium cation and metal anion on the reaction mechanism. The comparison of both approaches showed the advantages of microwave methodology in terms of efficiency and time saving. Indeed, the use of ground PET and microwave heating provided quantitative yields of BHET. Under conventional heating, the dinuclear iron complex gave slightly lower yield than (dimim)[FeCl₄] (74% vs 77% for post-consumer PET) after 24 h of reaction. However, the microwave-assisted process led to comparable results in remarkably shorter reaction times (2 h). Interestingly, complex **2**, containing the dipolar [Fe₂Cl₆(μ-O)]²⁻ moiety, provided higher yields than **1** with the non-dipolar [FeCl₄]⁻ anion (77% vs 69%). This behaviour has been rationalized on the basis of dielectric heating mechanisms (polarization and conduction), and it envisages a new approach towards more efficient catalysts by tailoring the catalytic species to be active under both heating mechanisms.

Keywords: Imidazolium-based halometallate complex • Iron-containing ionic liquid • Poly(ethylene terephthalate) • Bis(2-hydroxyethyl)terephthalate • Glycolysis.

INTRODUCTION

Nowadays, plastic has become an essential material in our daily life.¹ Among the different types of plastics, polyethylene terephthalate (PET) is one of the most widely used polymers.² The broad industrial interest in PET lies in its easy and low fabrication cost and attractive properties, such as

^a *Universidad de Cantabria, CITIMAC, Facultad de Ciencias, Avda. de los Castros s/n, 39005 Santander, Spain.*

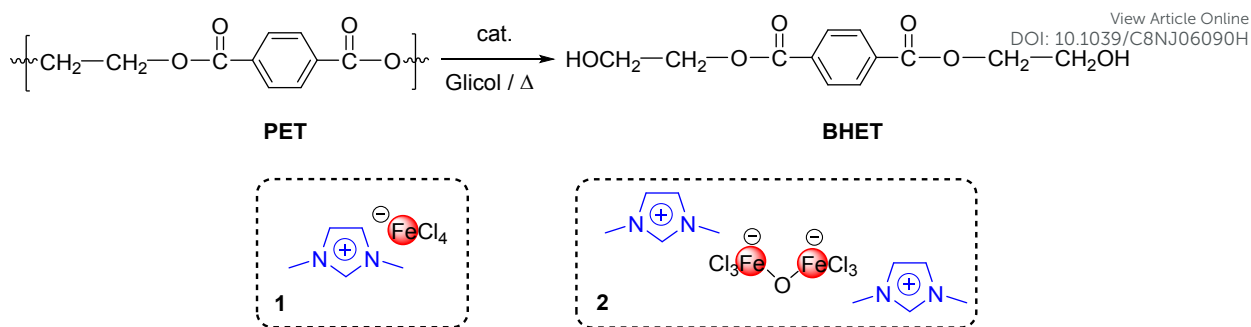
^b *GSK Carbon Neutral Laboratory for Sustainable Chemistry, University of Nottingham, NG7 2GA, Nottingham, UK*

^c *Universidad del País Vasco, Departamento de Química Inorgánica, Facultad de Ciencia y Tecnología, Apartado 644, E-48080, Bilbao, Spain.*

† Electronic supplementary information (ESI) available: Crystallographic data, analytical and spectral data.

thermal stability or malleability. These features make PET an ideal candidate to prepare a wide range of consumer products with applications in our society as, for example, packaging, adhesives or fibres, among others.² Indeed, the worldwide production of PET is higher than 50 million tons per year.³ However, the durability of PET due to its high stability and slow degradation make this polymer problematic at the end of its life phase. Consequently, plastic waste derived from PET-based products constitutes an important environmental problem and thus the development of more efficient recycling processes (chemical or physics) has become in an important research area.²⁻⁴ In this context, catalytic glycolysis is considered a powerful strategy for PET degradation.⁵ This simple strategy presents great advantages over other chemical methods (hydrolysis, methanolysis, and aminolysis)^{6,7} as, for example, low cost and production of pure monomer precursor that can be reused. The catalytic glycolysis consists in the depolymerization of PET into the monomer precursor, (bis(2-hydroxyethyl) terephthalate) or BHET, in the presence of a glycol at high temperatures by the use of an appropriate catalyst such as metal salts, nanocomposites or metal oxides, to name a few.^{2,4,7,8} In particular, ionic liquids (ILs) combine multiples and interesting features (*e.g.*, good thermal stability, non-volatility, and ease catalyst recovery and product purification) that make them suitable catalysts for this type of process.^{7,8b,9,10} Specifically, metal-containing ILs have shown a particular ability to perform this transformation. This type of bifunctional catalysts, containing a Lewis acid and a nucleophile within the structure, lead to better activities and selectivities than those observed by the use of simple metal salts or purely organic ILs. However, since the pioneering work of Zhang and Li,¹¹ who reported the use of paramagnetic Fe-based IL (bmim)[FeCl₄]¹² (bmim = 1-butyl-3-methylimidazolium) as catalyst for PET degradation, only a few examples have been described in the literature where halometallate-based ILs were employed as catalyst for glycolysis of PET.¹³ Among them, (bmim)₂[CoCl₄] and (bmim)₂[ZnCl₄] showed the highest catalytic activity reported to date (up to 99 % conversion of PET and 77-78 % selectivity of BHET) at 170 °C and 4 h.¹⁴

Inspired by these works, we set out to develop new bifunctional catalysts based on imidazolium type ILs containing halometallate for the glycolysis of PET. Specifically, herein we describe the preparation and catalytic applications of two imidazolium based halometallate complexes (Scheme 1): the mononuclear 1,3-dimethylimidazolium tetrachloridoferrate(III) complex, (dimim)[FeCl₄]¹⁵ (**1**), and the dinuclear 1,3-dimethylimidazolium (μ -oxido)bis[trichloridoferrate(III)] complex, (dimim)₂[Fe₂Cl₆(μ -O)] (**2**). The catalytic behaviour of these complexes was compared in the degradation of PET either under conventional or microwave-assisted heating conditions, which also enabled us to study the influence of the structure on the catalytic activity and contrast both methodologies.



Scheme 1 Glycolysis of PET catalysed by the new presented iron complexes **1** and **2**.

EXPERIMENTAL SECTION

General Procedures

Solvents were purchased from Sigma-Aldrich as HPLC grade. All reagents were purchased from Sigma Aldrich and purified when required by literature procedures.¹⁶ Chemical shifts of ¹H and ¹³C NMR are reported in ppm, the solvent was used as internal standard. Signals are quoted as s (singlet), d (doublet) and t triplet). Elemental analysis of **2** was performed employing a Euro EA Elemental CHNS rapid analyzer and an inductively coupled plasma atomic emission spectrometer (ICP-AES) from Perkin Elmer Analyst 100.

Nuclear magnetic resonance (NMR). ¹H and ¹³C NMR spectra were recorded on a Bruker DPX400 400 MHz and a DPX500 500 MHz nuclear magnetic resonance spectrometer.

Thermogravimetric analysis (TGA). Thermogravimetric measurements were carried out on a TA instruments Discovery at a heating rate of 10 °C/min and in a temperature range from 20 to 1000 °C under N₂ in a platinum crucible.

Differential scanning calorimetry (DSC). DSC measurements were carried out on a TA instruments Discovery from -90 to 150 °C at a rate of 10°C/min under nitrogen atmosphere.

Fourier transform infrared spectroscopy (ATR FT-IR). ATR FT-IR measurements were performed on a Bruker Alpha Series FT-IR spectrometer equipped with an attenuated total reflectance (ATR) module. The ATR FT-IR spectra were recorded by collecting 16 scans of a compound in the ATR module.

Electrospray ionization mass spectrometry (ESI-MS). ESI-MS analyses were carried out on a Bruker ESI-TOF MicroTOF II.

Gas chromatography mass spectrometry (GC-MS). GC-MS analyses of BHET product were performed on a Thermo Scientific ISQ-LT GC-MS equipped with a Single Quadrupole Mass Spectrometer and a ThermoScientific TG SQC column equivalent to DB5MS.

Single-crystal X-ray diffraction (SCXRD) and structure determination (CCDC: 1840841 and 1840842). The crystal structures of (dimim)₂[Fe₂Cl₆(μ-O)] (CCDC: 1840841) and the new polymorph of BHET (CCDC: 1840842) were determined by SCXRD. Data were collected using Cu-Kα radiation

(1.5418 Å) in an Agilent Technologies Supernova diffractometer. The data reduction was done with the CrysAlis PRO program.¹⁷ Data were corrected for Lorentz and polarization effects. All the structures were solved by direct methods using the SIR92 program¹⁸ and refined by full matrix least-squares on F^2 including all reflections (SHELXL97).¹⁹ All non-hydrogen atoms were refined anisotropically. H atoms were included at calculated positions and treated as riding atoms with isotropic thermal motion related to that of his parent atom. All calculations for these structures were performed using the WINGX crystallographic software package.²⁰ During the data reduction process of BHET, it became clear that the crystal specimen was twinned with twin law: (1.0003 0.0000 - 0.0008 / 0.3851 -1.0007 0.0009 / 0.4010 -0.0035 -1.0003). The final refinement showed a percentage for minor twin component of 34.8%. Crystallographic data and details of the structure determination and refinement for (dimim)₂[Fe₂Cl₆(μ-O)] (Tables S1† and S2†) and BHET product (Table S3†)) are summarized in the ESI†.

Crystallographic data for structures reported in this paper have been deposited in the Cambridge Crystallographic Data Center under reference numbers CCDC (1840841 and 1840842 for (dimim)₂[Fe₂Cl₆(μ-O)] and BHET, respectively). These data can be obtained free of charge via www.ccdc.cam.ac.uk/data_request/cif.

Powder X-ray data collection (PXRD). PXRD studies were performed in air atmosphere with the sample placed in an Anton Paar XRK 900 reactor chamber on a Bruker D8 Advance diffractometer with DAVINCI design, using Cu K_α radiation and a LynxEye detector. Diffraction patterns were collected at 300 °C in the 5–90° 2θ range with a step of 0.033° and a counting time of 0.8 s/step. The PXRD analysis (profile matching) in this work was carried out using the FullProf Suite.²¹

Density-functional theory calculations. Dispersion-corrected density-functional theory (DFT) calculations were performed using the code DMOL3 included in the BIOVIA “Materials Studio” package.²² The B3LYP²³ exchange-correlation functional was used in the calculations, together with the semiempirical dispersion correction scheme proposed by Tkatchenko-Sheffler.²⁴ Electric dipolar moment of the geometrically optimized structure of [Fe₂(μ-O)Cl₆]²⁻ anion was calculated from the partial charges computed using the ESP method as described by Singh and Kollman.²⁵

Synthetic Procedures

Synthesis of imidazolium-based halometallate complex (dimim)[FeCl₄] (1). Complex (dimim)[FeCl₄] (1) was obtained through a heat-assisted solvent-free reaction of a stoichiometric mixture of FeCl₃ and (dimim)Cl in a glove-box.¹⁵

Synthesis of imidazolium-based halometallate complex (dimim)₂[Fe₂Cl₆(μ-O)] (2). Freshly prepared (dimim)[FeCl₄] (0.4 mmol, 0.117 g) was suspended in 3 ml of methanol:heptanol (1:1) and the resulting mixture was stirred until total dissolution. Thereafter, H₂O (0.2 mmol, 3.2 μL) and triethylamine (Et₃N, 0.4 mmol, 55.4 μL) were added under continuous agitation and the mixture was stirred for 2 h.²⁶ The resulting reaction provided an orange precipitate corresponding to

(dimim)₂[Fe₂Cl₆(μ-O)] (0.054 g, yield: 92%). Single-crystals suitable for X-ray diffraction were grown by recrystallization in methanol (10 mL) at 5 °C. The resulting prismatic orange crystals were separated from the mother-liquor and washed with hexane. The purity of the prepared bulk samples was assessed by elemental analysis and X-ray diffraction measurements. Profile fitting of the diffraction patterns showed good agreement with the simulated one, while unindexed peaks were not observed. Elemental analysis: C₁₀H₁₈Cl₆Fe₂N₄O Calcd: C, 22.46; H, 3.39; Fe, 20.89; N, 10.48%; found C, 22.30; H, 3.56; Fe, 20.24; N, 10.60%.

Synthesis of imidazolium-based halometallate complex (mendimim)[FeCl₄]. The procedure was similar to the synthesis of **1**.¹⁵ Complex (mendimim)[FeCl₄] was obtained through a solvent-free reaction of a stoichiometric mixture of FeCl₃ and 1-((1*S*,2*R*,4*S*)-(+)-menthoxyethyl)-2,3-dimethylimidazolium chloride²⁷ ((mendimim)Cl) at 100 °C for 4 h. After cooling down to room temperature (R.T.), the final product was obtained as a grey-black solid. Elemental analysis: C₁₆H₂₉N₂OFeCl₄ Calcd: C, 41.50; H, 6.31; N, 6.05; Fe, 12.06%; found C, 44.32; H, 6.99; N, 7.01; Fe, 11.54%.

Catalytic Experiments

General procedure for catalytic degradation of PET by thermal heating. Protocol adapted from references 11, 13b and 14. In a typical experiment, the chosen amount of catalyst, 125 mg of PET (commercial pellets or PET waste) and 0.8 mL of EG, were placed in a 10 mL round bottom flask equipped with a reflux condenser. The mixture was heated under reflux at 170 °C for 24 h. After the specified time, the flask was cooled down R.T. and 50 mL of distilled water were added to the reaction crude. The undepolymerized PET was separated from the resulting mixture and dried at 80 °C. The mixture was filtered and the liquid phase was evaporated at 72 mbar using a rotary evaporator at 40 °C to remove water. An aliquot of the residue (100 mg) was dissolved in DMSO-d₆ and analyzed by ¹H and ¹³C NMR to determine the amount of BHET product using 1-phenyl-1,2-ethanediol (0.1 mmol) as internal standard. Afterwards, 3.5 mL of distilled water were added to the residue and the resulting solution was kept overnight in the fridge at 4 °C, obtaining white crystals of BHET, suitable for powder X-ray diffraction. Apart from the polymorph (*P2₁/a*) described in the literature, we were able to isolate a new polymorph of BHET as good quality crystals by slow evaporation at 5 °C in a methanolic solution.

General procedure for microwave-assisted catalytic degradation of PET. PET degradation experiments were carried out in a microwave reactor (CEM Corporation) equipped with a digital temperature control system and pressure sensors. In a typical experiment, the chosen amount of catalyst, 125 mg of PET (commercial pellets or PET waste) and 0.8 mL of EG, were placed in a 10 mL vessel. The reaction vial was sealed with a cap, introduced in the microwave reaction and the desired method was applied.

Two different methods were programmed in the microwave reactor, which enable to control how the system applies the microwave energy to the reaction:

- Standard Control: The microwave reactor applies the required power to maintain the reaction mixture at the desired temperature (170 °C) for a specified amount of time.
- Fixed Power Control: The microwave reactor applies a specified power (100 W) for a specified amount of time. A maximum temperature (170 °C) alters instrument operation, either by ending the irradiation cycle or by adjusting the power, if this temperature is reached.

After the specified time, the reaction vessel was automatically cooled down to R.T. and 50 mL of distilled water were added to the reaction crude. The undepolymerized PET was separated from the resulting mixture and dried at 80 °C. The mixture was filtered and the liquid phase was evaporated at 72 mbar using a rotary evaporator at 40 °C to remove water. An aliquot of the residue (100 mg) was dissolved in DMSO-*d*₆ and analyzed by ¹H and ¹³C NMR to determine the amount of BHET product using 1-phenyl-1,2-ethanediol (0.1 mmol) as internal standard. Afterwards, 3.5 mL of distilled water were added to the residue and the resulting solution was kept overnight in the fridge at 4 °C, obtaining white crystals of BHET suitable for SCXRD.

The conversion of PET is calculated using the following equation:

$$\text{Conversion of PET} = \frac{W_0 - W_1}{W_0} \times 100 \quad (1)$$

In which W_0 is the initial weight of PET and W_1 is the weight of undepolymerized PET. In addition, the yield and selectivity of BHET are defined by equations (2) and (3):

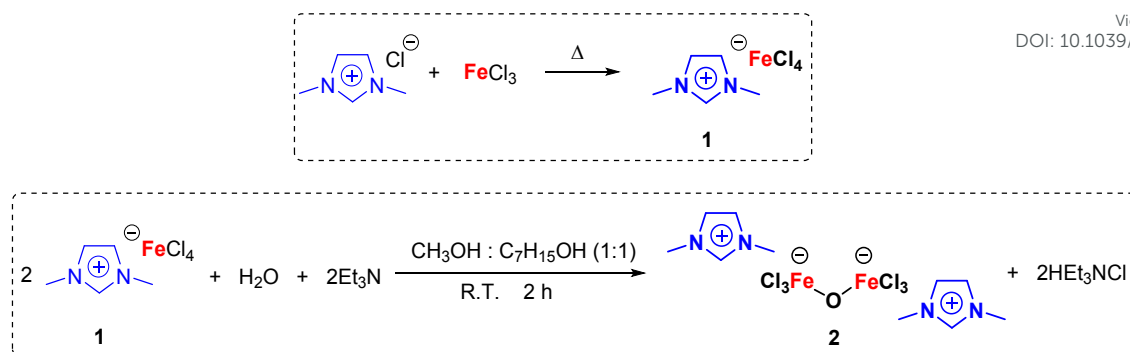
$$\text{Yield of BHET} = \frac{\text{moles of BHET}}{\text{initial moles of PET units}} \times 100 \quad (2)$$

$$\text{Selectivity of BHET} = \frac{\text{moles of BHET}}{\text{moles of depolymerized PET units}} \times 100 \quad (3)$$

RESULTS AND DISCUSSIONS

Characterization of Imidazolium-Based Halometallate Complexes (dimim)[FeCl₄] (1) and (dimim)₂[Fe₂Cl₆(μ-O)] (2)

The solvent-free reaction of FeCl₃ and (dimim)Cl affords the halometallate compound **1** (Scheme 2).¹⁵ The complex entity consists of [FeCl₄]⁻ anions in which the coordination polyhedral adopts a tetrahedral geometry. On the other hand, the imidazolium-based iron complex **2** was synthesized through addition of 0.5 eq. of H₂O and 1 eq. of Et₃N to a well-stirred solution of (dimim)[FeCl₄] in methanol:heptanol 1:1 (Scheme 2).²⁶



Scheme 2 Formation of (dimim)[FeCl₄] (**1**) and (dimim)₂[Fe₂Cl₆(μ-O)] (**2**) from FeCl₃ and (dimim)[FeCl₄] (**1**), respectively.

The structure of **2** was elucidated by single-crystal X-ray diffraction analysis. The crystal structure of compound **2** is built up by dinuclear (μ-oxido)bis(trichloridoferrate)(2-) anionic complexes and 1,3-dimethylimidazolium cations (Fig. 1, for further details see section 1, ESI†). The dinuclear iron complex presents similar structure to those of previously reported [Fe₂X₆(μ-O)]²⁻ type compounds (X: halide anion), showing a tetrahedral coordination environment around each metal center. The angular bridging oxide anion (Fe···O···Fe: 154.76 °; Fe···Fe: 3.472 Å) sets a staggered conformation between (FeCl₃) groups which results in a dinuclear complex anion that fits to C_s point group.²⁸ Note that in the crystal structure the oxygen atom is disordered over two symmetry-related positions with an occupancy factor of 0.5 each of them (Fig. 1 and section 1, ESI†).

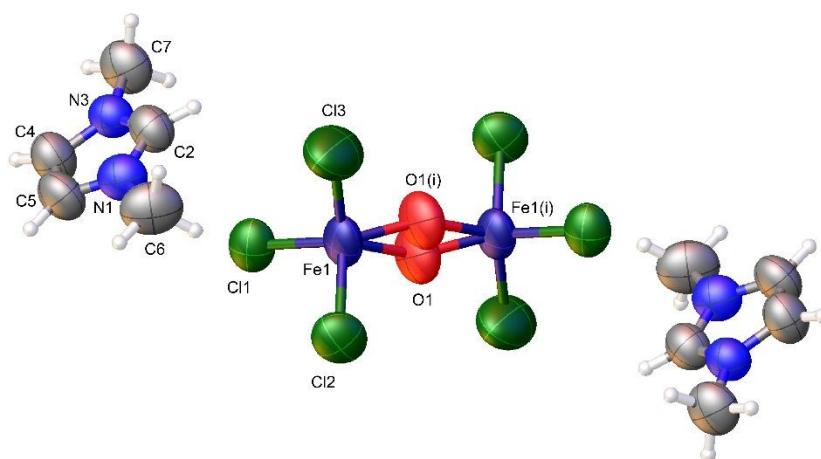


Fig. 1 X-ray molecular structure of (dimim)₂[Fe₂Cl₆(μ-O)] (**2**). Thermal ellipsoids are drawn at 50% probability. Selected bond lengths (Å) and angles (deg.) for [Fe₂Cl₆(μ-O)]²⁻: Fe1–O1 = 1.848(2), Fe1–Cl1 = 2.217(2), Fe1–Cl2 = 2.211(2), Fe1–Cl3 = 2.206(4), O1–Fe1–Cl1 = 103.1(6), O1–Fe1–Cl2 = 104.3(7), O1–Fe1–Cl3 = 124.5(5), Cl1–Fe1–Cl2 = 106.1(1), Cl1–Fe1–Cl3 = 110.3(1), Cl21–Fe1–Cl3 = 107.2(2).

Glycolysis of PET Catalysed by (dimim)[FeCl₄] and (dimim)₂[Fe₂Cl₆(μ-O)]

View Article Online
DOI: 10.1039/C8NJ06090H

Due to the particular ability of metal-containing ILs to depolymerize PET, we decided to evaluate the catalytic activity of (dimim)[FeCl₄] (**1**) and (dimim)₂[Fe₂Cl₆(μ-O)] (**2**) for the glycolysis of PET in ethylene glycol (EG), either under conventional heating or microwave-assisted conditions. Two different types of PET were employed: PET pellets purchased from Goodfellow Inc. (diameter 3–5 mm) and discarded commercial PET bottles acquired from local market, which were cut with a cutter to a maximum particle size of 6 mm. Through conventional heating, the optimal reaction conditions were found to be 0.8 mL of EG, 170 °C as a reaction temperature (160 °C inside the reaction flask) and a reaction time of 24 h. Table 1 reveals that there are differences in the catalytic behaviour of **1** and **2**. The glycolysis of PET catalysed by (dimim)[FeCl₄] was performed with quantitative conversion and all starting PET was degraded into oligomers, dimers and BHET, whereas the BHET product was obtained with high selectivity and yield (78%, entry 1). (dimim)₂[Fe₂Cl₆(μ-O)] was less active, probably due to a lower Brønsted basic character and/or higher steric hindrance (see “Degradation Mechanism of PET”), leading to the formation of BHET with 82% conversion and 54% yield (entry 2). The use of commercial PET in the reaction catalysed by **1** did not improve the results and the corresponding BHET product was obtained with analogous yield and selectivity (entry 3). However, we observed an increase in conversion, selectivity and yield for **2** when commercial PET was employed instead of PET pellets, achieving similar results to those provided by (dimim)[FeCl₄]. This correlates with the particle size of PET, since the smaller the size is, the higher the specific surface area of PET that could interact with EG and catalyst, thus resulting in an increase of activity. Indeed, the use of ground PET for **1** provided the BHET product with 93% yield and 94% selectivity, while the conversion was 99% (entry 5).

Table 1 Glycolysis of PET catalyzed by **1** and **2** under conventional heating.^a

Entry	Catalyst	PET	Conversion (%) ^b	Selectivity (%) ^c	Yield (%) ^c
1	1	pellets	>99	78	78
2	2	pellets	82	66	54
3	1	commercial	>99	77	77
4	2	commercial	96	76	74
5	1	ground PET	99	94	93

^a Reagents and conditions: **1** (0.085 mmol), **2** (0.0425 mmol), PET (125 mg), EG (0.8 mL), 170 °C, 24 h. ^b Conversion = $(W_0 - W_1) / W_0$, where W_0 is the initial weight of PET and W_1 is the weight of undepolymerized PET. ^c BHET determined through ¹H NMR spectroscopy by the use of 1-phenyl-1,2-ethanediol as internal standard (average of two runs).

Subsequently, we performed the catalytic degradation of PET applying microwave heating and retaining the same reaction parameters to those employed under conventional heating. The first set of experiments was conducted at a constant temperature of 170 °C (entries 1-6 in table 2). The system required 7 W to maintain the desired temperature in the reaction catalysed by (dimim)[FeCl₄], leading to the formation of BHET with 30% yield and 64% selectivity in 3 h, whereas the conversion was 47% (entry 1). (dimim)₂[Fe₂Cl₆(μ-O)] exhibited analogous catalytic performance (entry 2) as the previous one for a similar power (6.5 W). This contrasts with the degradation of PET catalysed by the metal precursor FeCl₃ for which 10 W were necessary, giving 15% yield and 95% selectivity of BHET (entry 3). Similarly, the imidazolium salt (dimim)Cl also showed less activity and required more energy (8 W) than **1** and **2** (entry 4). As expected, the use of PET taken from post-consumer bottles resulted in an improvement of yield and selectivity of BHET (~80% and 58%, respectively, entries 5 and 6). Furthermore, the conversion also increased notably.

Table 2 Microwave-Assisted glycolysis of PET catalyzed by **1** and **2**.^a

Entry	Catalyst	PET	Power (W)	t (h)	Conv. (%) ^b	Sel. (%) ^c	Yield (%) ^c
1	1	pellets	7	3	47	64	30
2	2	pellets	6.5	3	44	75	33
3 ^d	FeCl ₃	pellets	10	3	16	95	15
4 ^e	(dimim)Cl	pellets	8	3	6	90	5
5	1	commercial	7	3	76	78	58
6	2	commercial	6.5	3	75	80	58
7	1	pellets	100	2	42	76	32
8	2	pellets	100	2	62	82	50
9	1	commercial	100	2	>99	69	69
10	2	commercial	100	2	>99	77	77
11	1	ground PET	100	2	>99	>99	>99

^a Reagents and conditions: **1** (0.085 mmol), **2** (0.0425 mmol), PET (125 mg), EG (0.8 mL), 170 °C. ^b Conversion = $(W_0 - W_1) / W_0$, where W_0 is the initial weight of PET and W_1 is the weight of undepolymerized PET. ^c BHET determined through ¹H NMR spectroscopy by the use of 1-phenyl-1,2-ethanediol as internal standard (average of two runs). ^d 0.085 mmol FeCl₃. ^e 0.085 mmol (dimim)Cl.

Thereafter, a series of experiments were carried out at a constant microwave power of 100 W with a maximum temperature of 170 °C (entries 7-11 in table 2). An increase in the activity may be expected at higher irradiation power. Indeed, the glycolysis of PET pellets catalysed by (dimim)[FeCl₄] required less time (2 h) to give similar results to those observed in the experiment at constant

1
2
3 temperature (entries 1 and 7). 2 h of reaction under conventional heating led to the formation of
4 BHET with 5% conversion and 4% yield, proving the higher efficiency of microwave heating. View Article Online
DOI: 10.1039/C8NJ06090H
5
6 Interestingly, we noted an increased selectivity and yield for (dimim)₂[Fe₂Cl₆(μ-O)] (entry 8). In
7
8 addition, the glycolysis of commercial PET proceeded with quantitative conversion for both catalysts
9
10 (entries 9 and 10), while **2** showed higher yield and selectivity of BHET (77%) than **1** (69%).
11
12 Importantly, the use of ground PET provided quantitative formation of BHET (entry 11). The
13
14 advantages of microwave methodology in terms of efficiency and time saving is proved by the
15
16 comparison of results obtained through microwave-assisted conditions with those achieved under
17
18 conventional heating, for which 24 h of reaction are required for quantitative conversion of PET.

19
20 To understand the inversion on the catalytic activity order of **1** and **2** occurring upon the change of
21
22 heating source, the differences on the heating mechanisms must be considered. In conventional
23
24 heating, the energy is transferred from the surface of the reaction flask to inside and it is progressively
25
26 exchanged among all the species in the reaction mixture until a thermal equilibrium is reached. So
27
28 that, as previously mentioned, the greater catalytic activity of **1** by conventional heating can be related
29
30 to the sterically less hindered interaction that the mononuclear [FeCl₄]⁻ complex can establish with the
31
32 organic substrate (see “Degradation Mechanism of PET”). However, in the case of dielectric heating
33
34 the microwave irradiation penetrates in the material and transfers energy by direct coupling to the
35
36 solvent, substrate or catalyst molecules present in the reaction mixture, which undergo an increase of
37
38 temperature.²⁹ In this context, we must note that the dielectric heating courses through two main
39
40 mechanisms: dipolar polarization and ionic conduction. In the former, the dipole of a polar molecule
41
42 tends to align itself with the field via rotation and, as a result of the collisions taking place, the energy
43
44 is dissipated generating heat in the material. In ionic conduction mechanism, the influence of the
45
46 microwave electric field causes any mobile charged particles (e.g. ions, electrons) to move back and
47
48 forth through the material, heating the sample again due to collisions of charged species with adjacent
49
50 atoms or molecules. If we pay attention to the molecular geometry of **1** and **2**, the [FeCl₄]⁻ moiety of **1**
51
52 fits to an ideal T_d symmetry (Schönflies notation) which is incompatible with a permanent dipole
53
54 moment (i.e. μ = 0 D), despite molecular vibrations render transient minor polarity changes.
55
56 Consequently, direct heating of **1** involves only the ionic conduction mechanism. On the contrary, the
57
58 [Fe₂Cl₆(μ-O)]⁻ anion of **2** exhibits a C_s point group which sets a net dipole moment of μ = 0.623 D
59
60 (according to DFT calculations), allowing both heating mechanisms to take place and boosting its
catalytic performance in comparison to **1**.

A key attraction to the standpoint of environmental protection and the economics of the process is the
possibility of catalyst recovery and reuse. Therefore, we performed a number of experiments either
under conventional heating or microwave-assisted conditions in order to study the recyclability of the
complex (dimim)₂[Fe₂Cl₆(μ-O)]. Ultimately, **2** exhibits a limited potential for recyclability. Briefly, by
addition of water and subsequent centrifugation of the insoluble fraction, the dinuclear iron complex
could be recovered and used in successive cycles. However, a significant decrease in the activity was

observed in the second cycle (Fig. S1†), which is due to a gradual decomposition of **2** as a consequence of the repeated washing cycles. Indeed, further analyses revealed that **2** is decomposed by the addition of water (solvent employed in the work-up once finished the catalytic experiment). Finally, a set of experiments were carried out under conventional heating in order to determine the importance of both metal complexes to the observed catalytic activity (Table 3). First, no reaction was detected without catalyst (entry 3). Next, the use of glycerol instead of EG, with **2** as catalyst, led to similar observations, suggesting that EG is involved in the reaction mechanism (entry 4). Additionally, the imidazolium salt (dimim)Cl and the metallic precursor FeCl₃ were analyzed separately and both were less active than the metal complexes catalysts under the optimized reaction conditions (entries 5 and 6), in a similar way to microwave heating. These results reveal that both cation (dimim)⁺ and anion ([FeCl₄]⁻ and [Fe₂Cl₆(μ-O)]²⁻) belonging to the Fe-based ionic liquids play a key role in the glycolysis of PET, and thus proves the cooperative effect of the two moieties. We have also compared the activity and selectivity of **1** and **2** (entries 1 and 2) with those showed by the previously described (bmim)[FeCl₄] complex under similar reaction conditions (PET pellets of 3–5 mm purchased from Goodfellow Inc.; T = 170 °C, 160 °C inside the reaction flask).¹¹ The use of (bmim)[FeCl₄] as catalyst allowed a realistic estimation of the catalytic behaviour of **1** and **2**. Interestingly, we observed lower selectivity and yield for the former, giving 57 and 46%, respectively (entry 7). This comparison suggests that changes in the imidazolium cation can affect the catalytic activity. In particular, the improved activity and selectivity of **1** and **2** in comparison with those of (bmim)[FeCl₄] may be due to a higher steric hindrance for the later, and thus smaller cations favour the catalytic process (see “Degradation Mechanism of PET”). Indeed, the use of a new Fe-based ionic liquid (mendemim)[FeCl₄] containing an imidazolium cation which is even bulkier (1-menthoxymethyl-2,3-dimethylimidazolium) led to lower yield and selectivity of BHET (entry 8) than those observed for **1**, **2** and (bmim)[FeCl₄].

Table 3 Summary of the attempted glycolysis of PET using different catalytic systems.^a View Article Online
DOI: 10.1039/C8NJ06090H

Entry	Catalyst	Conversion (%) ^b	Selectivity (%) ^c	Yield (%) ^c
1	1	>99	78	78
2	2	82	66	54
3	--	0	0	0
4 ^c	2	0	0	0
5 ^d	(dimim)Cl	11	69	7
6 ^e	FeCl ₃	74	52	38
7	(bmim)FeCl ₄	81	57	46
8	(mendimim)[FeCl ₄]	82	46	37

^a Reagents and conditions: PET pellets (125 mg), EG (0.8 mL), 170 °C, 24 h. ^b Conversion = $(W_0 - W_1) / W_0$, where W_0 is the initial weight of PET and W_1 is the weight of undepolymerized PET. ^c BHET determined through ¹H NMR spectroscopy by the use of 1-phenyl-1,2-ethanediol as internal standard (average of two runs). ^c Glycerol as solvent, **2** (0.0425 mmol). ^d 0.165 mmol (dimim)Cl. ^e 0.165 mmol FeCl₃.

It is worth noting that the advantages of the presented materials over conventional catalysts such as metal acetates in the glycolysis of PET are: (i) the reaction rate is notably increased and (ii) the obtained BHET product could be obtained with higher purity (*vide infra*).

Characterization of BHET Product

The pure BHET product was obtained by the addition of water to the residue generated after work-up. The resulting solution was kept overnight in the fridge, obtaining white crystals of BHET. The purity of the BHET product was confirmed by the use of a wide range of techniques, such as PXRD, TGA, FT-IR, NMR, ESI-MS and GC-MS. Fig. 2 shows the PXRD data of BHET which has been fitted using the pattern matching routine and the cell parameters and the space group (P2₁/a) reported by S. Kashino et al. for a BHET polymorph.³⁰ The fitting yielded similar unit cell parameters to those previously reported [$a = 25.921(1)$, $b = 5.513(1)$ and $c = 8.584(1)$ Å with $\beta = 99.118(1)^\circ$] and any unmatched diffraction peak was observed in the final refinement, which confirms the existence of a pure crystal phase. In addition, the raw PET sample (see inset of fig. 2) exhibits a typical diffraction pattern of this polymer with a semicrystalline structure,³¹ featured by broad diffraction peaks at 2θ values of 16.4, 17.5, and 22.9 and 26.0°. Accordingly, non-traces of PET is observed in the PXRD pattern of BHET, which supports further its purity.

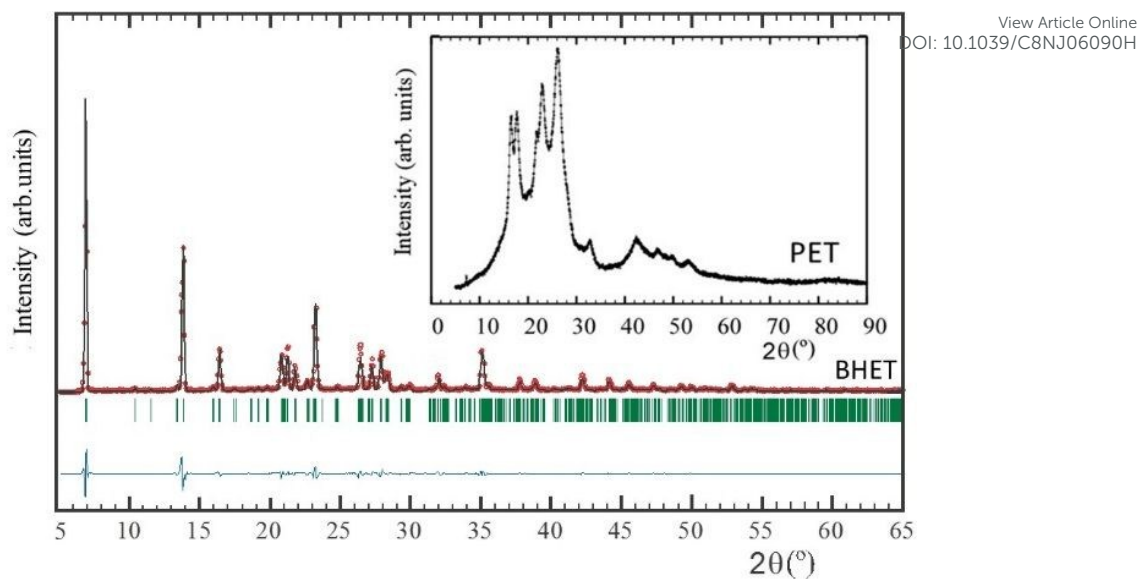


Fig. 2 Observed (red crosses), calculated (black solid line) and difference (blue solid line) PXRD patterns of BHET at R.T. Vertical marks correspond to the position of the allowed reflections for the crystallographic structure. The inset shows the observed PXRD pattern of PET at R.T.

The ^1H and ^{13}C NMR spectra exhibit the characteristic signals belonging to the BHET molecule,³² whereas no signals corresponding to other compounds were found (Fig. 3).

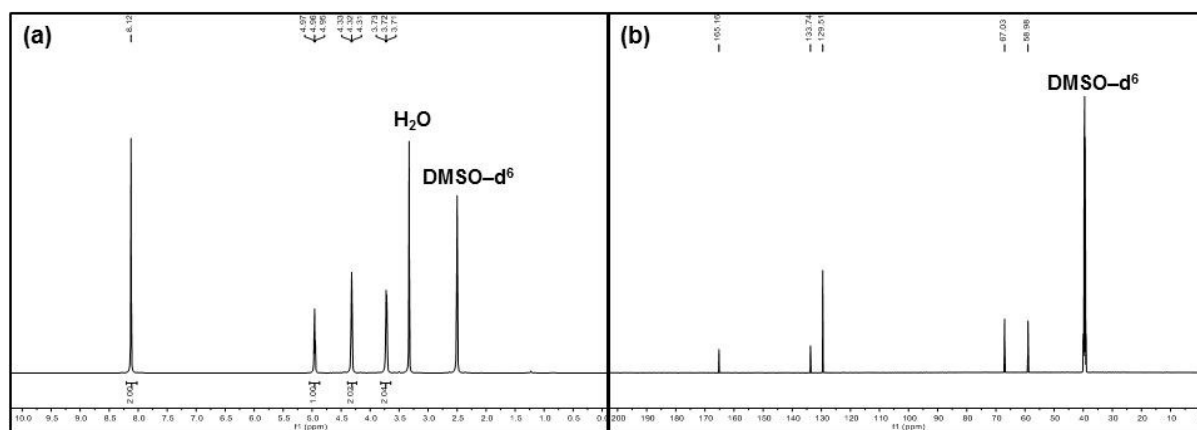
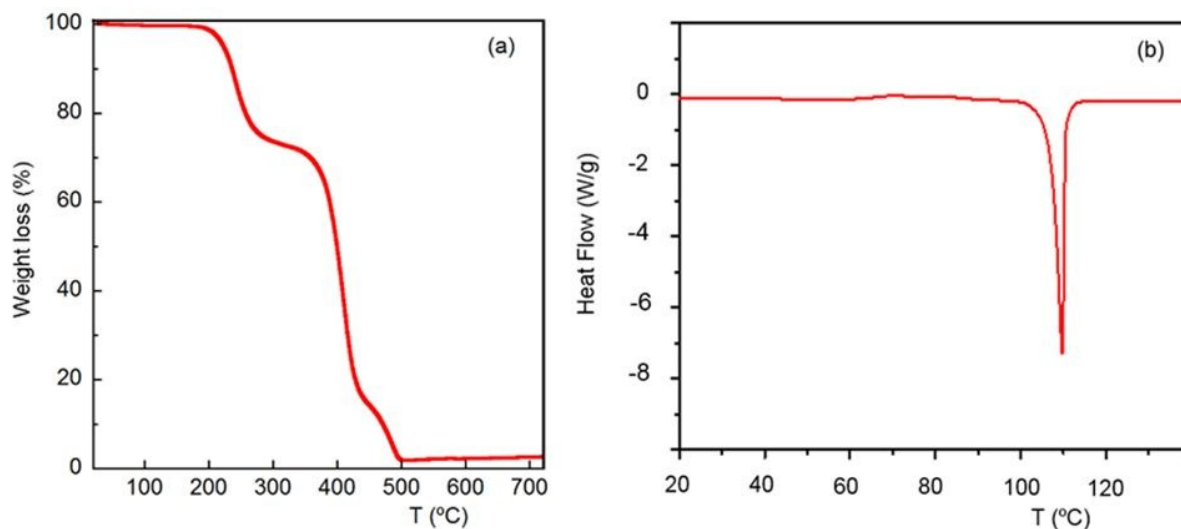


Fig. 3 NMR patterns of BHET product. (a) ^1H NMR (500 MHz, $\text{DMSO}-d_6$): δ 8.12 (s, 4H, CH_{Ar}), 4.96 (t, $J = 5.7$ Hz, 2H, $-\text{OCH}_2\text{CH}_2\text{OH}$), 4.32 (t, $J = 4.9$ Hz, 4H, $-\text{OCH}_2\text{CH}_2\text{OH}$), 3.72 (t, $J = 5.2$ Hz, 4H, $-\text{OCH}_2\text{CH}_2\text{OH}$). (b) ^{13}C NMR (126 MHz, DMSO): δ 165.2 (s, C_q , $\text{C}=\text{O}$), 133.7 (s, C_q , C_{Ar}), 129.5 (s, CH , C_{Ar}), 67.0 (s, $-\text{OCH}_2\text{CH}_2\text{OH}$), 59.0 (s, $-\text{OCH}_2\text{CH}_2\text{OH}$).

The obtained BHET was further analyzed by TGA and DSC. The TGA curve (Fig. 4a) displays one weight loss of around 31% at 228 $^\circ\text{C}$, corresponding to the thermal decomposition of BHET, and another weight loss of about 66% at 421 $^\circ\text{C}$, due to the thermal decomposition of PET repolymerized

1
2
3 during the heating carried out in the TGA study.^{13a,32,33} The DSC curve presents a sharp endothermic
4 peak at 109.7 °C, which is consistent with the reported melting point of BHET (Fig. 4b).^{29,34}
5
6
7

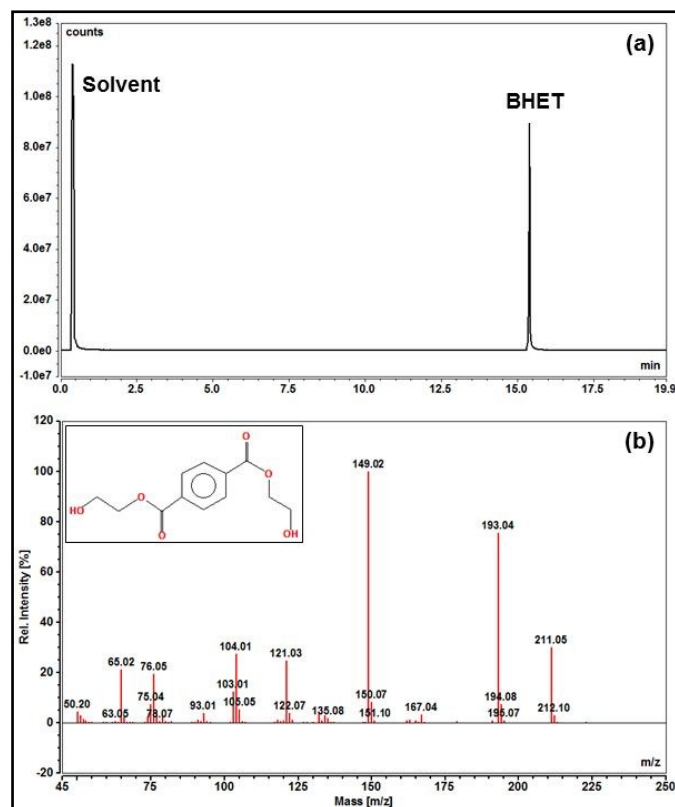


29
30
31
32
33
34
35
36
37
38
39
40
41
42
43
44
45
46
47
48
49
50
51
52
53
54
55
56
57
58
59
60

Fig. 4 (a) TGA and (b) DSC curves of BHET product.

The FTIR spectrum of the main product (Fig. S2†) is in good agreement with those described in the literature for BHET.³² The peaks at 3350 and 1140 cm^{-1} indicate the presence of hydroxyl groups (OH). The bands at 1720, 1258, and 1076 cm^{-1} are assigned to C=O, C–O ester bond asymmetric vibration, and C–O ester bond symmetric vibration, respectively. The signals between 890 and 670 cm^{-1} are attributed to the vibration of aromatic rings. In addition, the sharpness of FTIR peaks suggests high purity and crystallinity for the BHET obtained from the depolymerization process.

On the other hand, the purified BHET was also analyzed by ESI-MS and GC-MS. These techniques also proved that the main product was obtained with high purity, since no signals related to other compounds were observed. The ESI-MS spectrum (Fig. S3†) displays one main signal with m/z 277 and 100% intensity corresponding to BHET ionized by Na^+ . Two small peaks with m/z 255, 9.2% intensity and m/z 293, 10.8% intensity are also visible, which belong to BHET ionized by H^+ and K^+ , respectively.³⁵ In addition, the GC-MS spectrum reveals the presence of only one compound, which gives a peak at 15.39 min (Fig. 5a) attributable to the main product (Fig. 5b). The peak at 0.42 min corresponds to the solvent (acetonitrile). All of these data demonstrate that highly pure BHET was obtained once the crystallization process in water was performed.



View Article Online
DOI: 10.1039/C8NJ06090H

Fig. 5 GC-MS spectrum of BHET product: (a) GC spectrum; (b) MS spectrum.

Crystals of a new polymorph of BHET were isolated by slow evaporation of the obtained white crystals at 5 °C in methanol (Fig. 6, for further details see section 4, ESI†).³⁶ The new BHET polymorph crystallizes in the $P\bar{1}$ space group (see CIF file) and its crystallographic unit cell contains four independent BHET molecules (Fig. S4†). The crystal structure is sustained through a complex network of intermolecular hydrogen bonding interactions involving different groups (C=O, C–OH and C_{Ar}–H) and by π – π stacking between phenyl rings.

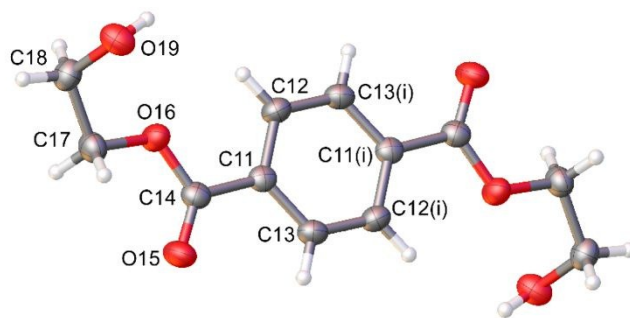
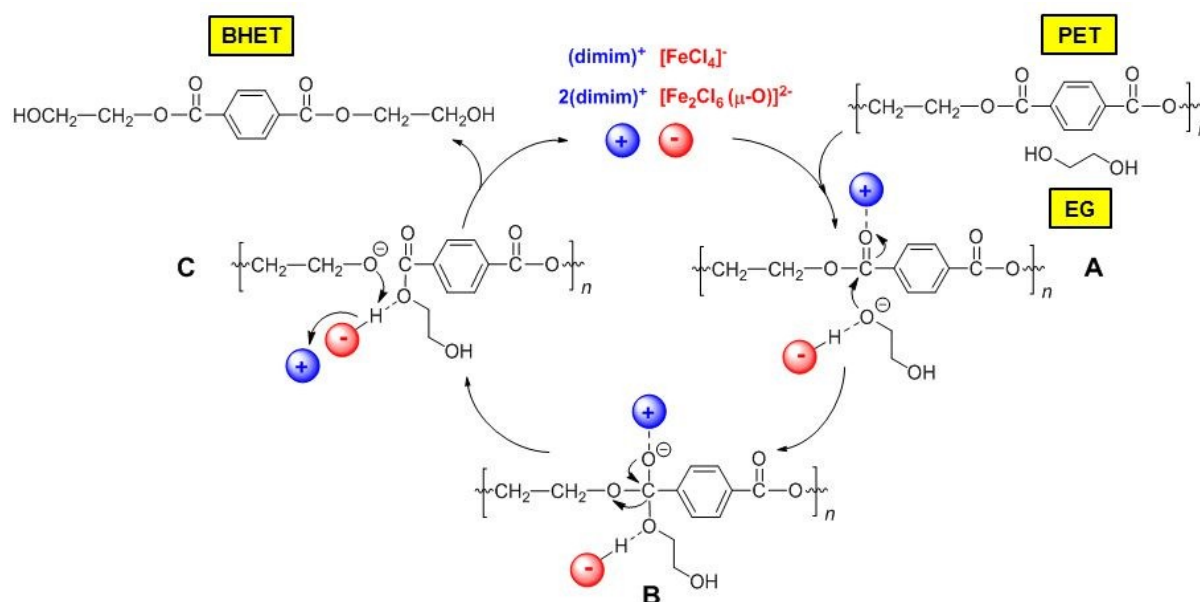


Fig. 6 Crystal structure of the new BHET ($P\bar{1}$) polymorph: BHET molecule showing the numbering scheme (i: -x, 1-y, 1-z). Thermal ellipsoids are drawn at 50% probability.

Degradation Mechanism of PET

View Article Online
DOI: 10.1039/C8NJ06090H

Based on literature reports, the reaction mechanism is a Lewis acid catalytic process^{11,13a} in which hydrogen-bonding interactions play an important role in the interaction of EG and the ester groups of PET (Scheme 3).^{8a,37} Both imidazolium cation and metal complex anion play a synergistic key role. The hydrogen atoms of imidazolium cation interact with the oxygen of the C=O group in the ester of PET (**A**). Consequently, a substituent with different bulkiness in the imidazolium cation can lead to a different catalytic activity (Table 3). Simultaneously, the anion ($[\text{FeCl}_4]^-/[\text{Fe}_2\text{Cl}_6(\mu\text{-O})]^{2-}$) attacks the hydrogen atom of $-\text{OH}$ functionality in EG through intermolecular hydrogen-bonding interactions, making the oxygen of this group more negative (Scheme 3). As a consequence, this oxygen is more prone to interact with the electrophilic carbon of the ester group in PET and render the formation of a tetrahedral carbocation intermediate (**B**). The $[\text{FeCl}_4]^-$ anion exhibits slightly higher activity than $[\text{Fe}_2\text{OCl}_6]^{2-}$ moiety under conventional heating, probably due to a higher steric impediment in the latter. However, as previously mentioned, under dielectric heating conditions the performance of **2** surpasses that of **1**, since the dipolar $[\text{Fe}_2\text{OCl}_6]^{2-}$ entity interacts with the microwave field through both mechanisms, dipolar polarization and ionic conduction, boosting as consequence the reaction (note that the $[\text{FeCl}_4]^-$ ion lacks a permanent electric dipole moment and ideally the dielectric heating takes place only through the ionic conduction mechanism). Finally, the cleavage of the C–O bond is promoted (**C**), and oligomers, dimers, and monomers are generated sequentially.



Scheme 3 Proposed mechanism for the glycolysis of PET.

CONCLUSIONS

View Article Online
DOI: 10.1039/C8NJ06090H

In summary, we have successfully employed two imidazolium based halometallate complexes, $(\text{dimim})_2[\text{Fe}_2\text{Cl}_6(\mu\text{-O})]$ and $(\text{dimim})[\text{FeCl}_4]$, as catalysts for the glycolysis of PET, either under conventional heating or microwave-assisted conditions. Quantitative conversions of PET and high yields of BHET were observed through the two approaches, but a comparison of results obtained by microwave-assisted conditions with those achieved under conventional heating showed the benefits of microwave methodology in terms of efficiency and time saving. Indeed, the use of ground PET under microwave heating provided quantitative formation of BHET.

$(\text{dimim})_2[\text{Fe}_2\text{Cl}_6(\mu\text{-O})]$ afforded lower yields than $(\text{dimim})[\text{FeCl}_4]$ by conventional heating both for post-consumer and purchased PET, probably due to the steric effect generated by the more bulky $(\mu\text{-oxido})\text{bis}(\text{trichloridoferrate})$ anion. However, the dinuclear iron dimer showed higher catalytic activity than the monoatomic complex under microwave-assisted conditions because of the more efficient dielectric heating taking place upon the dipolar metal complex present in $(\text{dimim})_2[\text{Fe}_2\text{Cl}_6(\mu\text{-O})]$. A more generic conclusion of this result envisages a new approach to develop more efficient catalysts under microwave assisted conditions by tailoring the catalytic species to be active under both dielectric heating mechanisms (polarization and ion conduction). The study also suggested that the bulkiness of the imidazolium cation affect the catalytic activity in such a way that smaller cations favour the catalytic process. Similarly, the cooperative effect of the two moieties of the catalyst, cation $(\text{dimim})^+$ and anion ($[\text{FeCl}_4]^-$ and $[\text{Fe}_2\text{Cl}_6(\mu\text{-O})]^{2-}$), was further supported by additional experiments. Finally, the crystal structure of a new polymorph of BHET was isolated, which can be of interest for the scientific community and polymer industry, since polymorphic forms of a substance can exhibit different properties in terms of chemical reactivity, apparent solubility, melting point, vapor pressure, and density.

In conclusion, this study has evidenced the suitability of the microwave radiation as a powerful technique for degradation of PET compared to conventional heating. Furthermore, two new halometallate complexes has been added to the toolbox of PET glycolysis with metal-containing ILs, for which the structure of halometallate moieties and the steric hindrance provoked by bulky ions could be key and thus may inspire the design of new catalysts that exhibit an improved catalytic performance.

AUTHOR INFORMATION

Corresponding Authors

*E-mail: israel.canorico@nottingham.ac.uk (Israel Cano)

*E-mail: depedrov@unican.es (Imanol de Pedro)

ORCID

Israel Cano: 0000-0003-3727-9327

Imanol de Pedro: 0000-0002-5581-2220

View Article Online
DOI: 10.1039/C8NJ06090H

CONFLICTS OF INTEREST

There are no conflicts of interest to declare.

ACKNOWLEDGMENTS

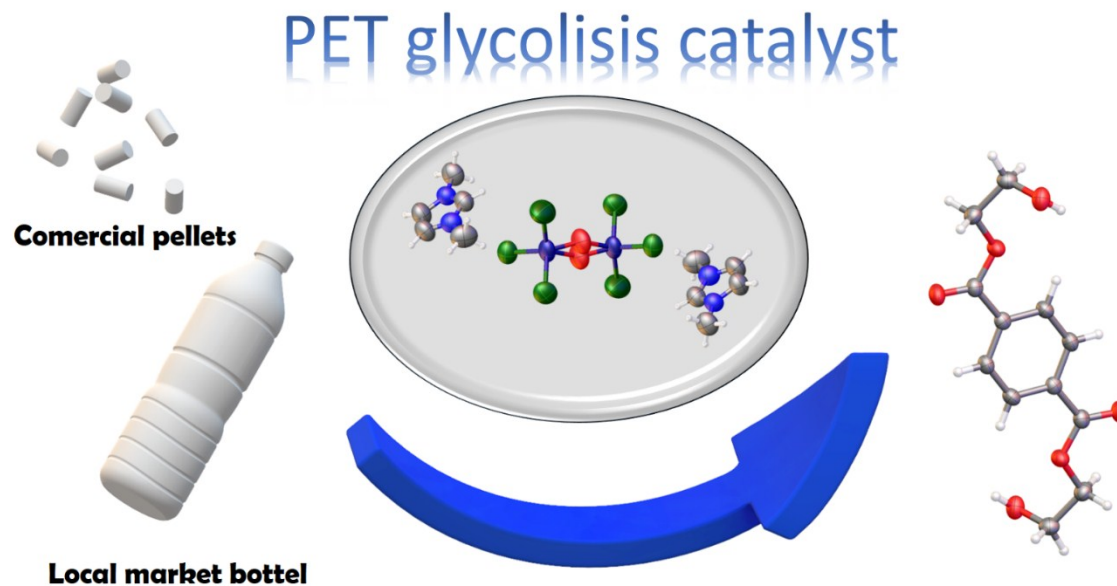
Financial support from the Spanish Ministerio de Ciencia e Innovación (Projects MAT2014-55049-C2-R and MAT2016-75883-C2-1-P), Universidad del País Vasco/Euskal Herriko Unibertsitatea (GIU17/50 and PPG17/37). Universidad de Cantabria (Proyecto Puente convocatoria 2018 financed by SODERCAN-FEDER). The authors also gratefully acknowledge Technical and human support provided by SGIKER (UPV/EHU, MINECO, GV/EJ, ERDF, and ESF). Israel Cano acknowledges financial support from the European Union's Horizon 2020 research and innovation programme through a Marie Skłodowska-Curie Individual Fellowship (IF-EF; Programme/Call: H2020-MSCA-IF-2015; Proposal No: 704710–Sdchirnanocat).

NOTES AND REFERENCES

- 1 A. Lusher, P. Hollman and J. Mendoza-Hill, Microplastics in fisheries and aquaculture: status of knowledge on their occurrence and implications for aquatic organisms and food safety, *FAO Fisheries and Aquaculture Technical Paper*, 2017, **615**.
- 2 L. Bartolome, M. Imran, B. G. Cho, W. A. Al-Masry and D. H. Kim, in *Recent Developments in the Chemical Recycling of PET, Material Recycling - Trends and Perspectives*, ed. D. Achilias, InTech, Rijeka (Croatia), 2012, pp. 65–84.
- 3 U. T. Bornscheuer, *Science*, 2016, **351**, 1154–1155.
- 4 A. M. Al-Sabagh, F. Z. Yehia, Gh. Eshaq, A. M. Rabie and A. E. El Metwally, *Egypt. J. Pet.*, 2016, **25**, 53–64.
- 5 K. Troev, G. Grancharov, R. Tsevi and I. Gitsov, *J. Appl. Polym. Sci.*, 2003, **90**, 1148–1152.
- 6 V. Sinha, M. R. Patel and J. V. Patel, *J. Polym. Environ.*, 2010, **18**, 8–25.
- 7 N. George and T. Kurian, *Ind. Eng. Chem. Res.*, 2014, **53**, 14185–14198.
- 8 (a) Q. Wang, X. Yao, S. Tang, X. Lu, X. Zhang and S. Zhang, *Green Chem.*, 2012, **14**, 2559–2566; (b) B. Geyer, G. Lorenz and A. Kandelbauer, *EXPRESS Polym. Lett.*, 2016, **10**, 559–586.
- 9 (a) J. P. Hallett and T. Welton, *Chem. Rev.*, 2011, **111**, 3508–3576; (b) C. Jehanno, I. Flores, A. P. Dove, A. J. Müller, F. Ruipérez and H. Sardon, *Green Chem.*, 2018, **20**, 1205–1212.
- 10 (a) H. Wang, Y. Liu, Z. Li, X. Zhang, S. Zhang and Y. Zhang, *Eur. Polym. J.*, 2009, **45**, 1535–1544; (b) H. Wang, Z. Li, Y. Liu, X. Zhang and S. Zhang, *Green Chem.*, 2009, **11**, 1568–1575.
- 11 H. Wang, R. Yan, Z. Li, X. Zhang and S. Zhang, *Catal. Comm.*, 2010, **11**, 763–767.

- 12 K. Bica and P. Gaertner, *Org. Lett.*, 2006, **8**, 733–735.
- 13 (a) X. Zhou, X. Lu, Q. Wang, M. Zhu and Z. Li, *Pure Appl. Chem.*, 2012, **84**, 789–801; (b) Q. Wang, X. Lu, X. Zhou, M. Zhu, H. He and X. Zhang, *J. Appl. Polym. Sci.*, 2013, **129**, 3574–3581; (c) Q. F. Yue, L. F. Xiao, M. L. Zhang and X. F. Bai, *Polymers*, 2013, **5**, 1258–1271.
- 14 Q. Wang, Y. Geng, X. Lu and S. Zhang, *ACS. Sustain. Chem. Eng.*, 2015, **3**, 340–348.
- 15 A. García-Saiz, P. Migowski, O. Vallcorba, J. Junquera, J. A. Blanco, J. A. González, M. T. Fernández-Díaz, J. Rius, J. Dupont, J. Rodríguez-Fernández and I. de Pedro, *Chem. Eur. J.*, 2014, **20**, 72–76.
- 16 W. L. F. Armarego and D. D. Perrin, *Purification of Laboratory Chemicals*, Butterworth-Heinemann, Oxford (UK), 1997.
- 17 Oxford Diffraction CrysAlis CCD & CrysAlis RED. Version 1.171.29. Oxford Diffraction Ltd, Wrocław, 2006, Poland.
- 18 A. Altomare, G. Cascarano, C. Giacovazzo and A. Guagliardi, *J. Appl. Cryst.*, 1993, **26**, 343–350.
- 19 G. M. Sheldrick, *Acta Cryst.*, 2008, **A64**, 112–122.
- 20 L. J. Farrugia, *J. Appl. Cryst.*, 1999, **32**, 837–838.
- 21 J. Rodríguez-Carvajal, FULLPROF program for rietveld refinement and pattern matching analysis of powder patterns, *Phys. B* 1993, **192**, 55–69; and unpublished later versions. The program is a strongly modified version of that described by D. B. Wiles and R. A. Young, *J. Appl. Cryst.*, 1981, **14**, 149–151.
- 22 Materials Studio, R2; BIOVIA, 2017.
- 23 A. D. Becke, *J. Chem. Phys.*, 1993, **98**, 5648–5652.
- 24 A. Tkatchenko and M. Scheffler, *Phys. Rev. Lett.*, 2009, **102**, 073005.
- 25 U. C. Singh and P. A. Kollman, *J. Comput. Chem.*, 1984, **5**, 129–145.
- 26 W. A. Hermann, in *Synthetic Methods of Organometallic and Inorganic Chemistry*, Georg Thieme Verlag, Stuttgart (Germany), 1996, p. 144–145.
- 27 S. Mumtaz, I. Cano, N. Mumtaz, A. Abbas, J. Dupont and H. Y. Gondal, *Phys. Chem. Chem. Phys.*, 2018, **20**, 20821–20826.
- 28 (a) G. Haselhorst, K. Wieghardt, S. Keller and B. Schrader, *Inorg. Chem.*, 1993, **32**, 520–525; (b) X. Wang, S. Wang, L. Li, E. B. Sundberg and G. P. Gacho, *Inorg. Chem.*, 2003, **42**, 7799–7808; (c) J.-C. Chang, W.-Y. Ho, I.-W. Sun, Y.-K. Chou, H.-H. Hsieh, T.-Y. Wu and S.-S. Liang, *Polyhedron*, 2010, **29**, 2976–2984.
- 29 (a) N. Pingale and S. Shukla, *Eur. Polym. J.*, 2008, **44**, 4151–4156; (b) J. Sun, W. Wang and Q. Yue, *Materials*, 2016, **9**, 231.
- 30 S. Kashino and M. Haisa, *Acta Cryst.*, 1975, **B31**, 1819–1822.
- 31 S. D. Gates, T. N. Blanton and T. G. Fawcett, *Powder Diffrac.*, 2014, **29**, 102–107.

- 32 D. S. Achilias, H. H. Redhwi, M. N. Siddiqui, A. K. Nikolaidis, D. N. Bikiaris and G. P. Karayannidis, *J. Appl. Polym. Sci.*, 2010, **118**, 3066-3073.
- 33 C. H. Chen, *J. Appl. Polym. Sci.*, 2003, **87**, 2004–2010.
- 34 C. H. Chen, C. Y. Chen, Y. W. Lo, C. F. Mao and W. T. Liao, *J. Appl. Polym. Sci.*, 2001, **80**, 943–948.
- 35 The presence of Na⁺ is due to the use of sodium formate as a calibration compound for the mass scale, which is introduced before every sample run. Na and K can also be sourced from glassware.
- 36 The structure of an additional second polymorph (*P*₂*1*₂*1*₂*1*) is described by the Cambridge Structural Database: W. McDonald, E. Lewis and D. Bower, *Acta Cryst.*, 1983, **C39**, 410–412.
- 37 J. Sun, D. Liu, R. P. Young, A. G. Cruz, N. G. Isern, T. Schuerg, J. R. Cort, B. A. Simmons and S. Singh, *ChemSusChem*, 2018, **11**, 781–792.



Tailoring halometallate-based ionic liquids (bulkiness and polarization) to be more active catalysts for PET glycolysis under conventional and microwave-assisted heating